

A RADIOMETRY METHOD OF DETERMINING THE SUBSOIL TEMPERATURE  
PROFILE AND DEPTH OF SOIL FREEZING

K. P. Gaikovich, A. N. Reznik, and R. V. Troitskii

UDC 621.371:551.526

We present results from theoretical and experimental studies into the possibilities of thermal probing of soil by means of a microwave radiometry method. A special measurement method has been developed to eliminate the effect of the reflective and scattering characteristics of the soil on radio emissions. Subsoil temperature profiles have been reproduced on the basis of measurement data from thermal radio emissions under summer and winter conditions at wavelengths of 0.8, 3, 9, and 13 cm, and the daily dynamics of soil temperature were investigated. Methods have been developed for the determination of the extent to which the soil is frozen, and the accuracy of these methods was 15-20%.

Long-range determination of a vertical temperature profile through the thickness of soil offers opportunities of studying the thermal regime of a soil without violating its structural integrity, of studying the processes of heat exchange in the underlying surface and the atmosphere, of determining the depths of soil freezing and ice thicknesses, of observing deep thermal anomalies associated with underground fires, volcanic activity, the movement of heat (including observation of discontinuities), etc. Long-range thermal probing becomes possible on the basis of multi-frequency radiometry measurements, with subsequent solution of the corresponding inverse problem. The probing is accomplished to the depth of the skin layer, which in the DM range goes from several centimeters in the moist soils to several meters in dry soils or in frozen soils [1]. The formulated problem has been studied from the theoretical standpoint, for example, in [2, 3]; however, this method has found no practical application as of the present time, a situation which can be ascribed to the great difficulty in controlling the effect of competing factors on the brightness temperature of the soils, and namely: surface reflection, as well as scattering from three-dimensional and surface nonhomogeneities. A special measurement method is employed in this study to eliminate the effect of the above-enumerated factors on thermal radio emission. Methods have been developed to solve the reciprocal problems of reproducing the temperature profile. As a result, soil temperature profiles have been obtained experimentally under various physical conditions, and a radiometry method for the determination of the extent to which the soil has been frozen has been developed on this basis.

1. Measurement Method. When the effect of reflection and scattering is offset, most favorable conditions arise for radio methods of thermal probing of media. In this case, the spectral relationship  $T_b(\lambda)$  is governed only by the non-homogeneity of the temperature profile  $T(z)$ . A compensation method is used in this study which involves the positioning of the reception antenna beneath a reflective shield (see Fig. 1). This method was used successfully in [4] to probe a water medium; however, its applicability in the study of soils requires special study.

The effectiveness of the method for isothermal distribution of temperature  $T(z) = T_0 = \text{const}$  is obvious. In this case, according to [5], the intensity of the thermal radiation from an absorbing half-space is proportional to the absorbed power of the auxiliary plane wave incident out of a transparent medium. In the presence of a reflecting shield, the entire power is absorbed and therefore we have  $T_b = T_0$ . In the case of a non-isothermal profile the problem becomes more complex.

Let us examine a random-non-homogeneous radiating half-space with dielectric permittivity  $\epsilon = \epsilon_0 + \tilde{\epsilon}(r)$ , where  $\langle \epsilon \rangle = \epsilon_0 = \epsilon' - i\epsilon''$ , while  $\tilde{\epsilon}$  is a statistical uniform random function

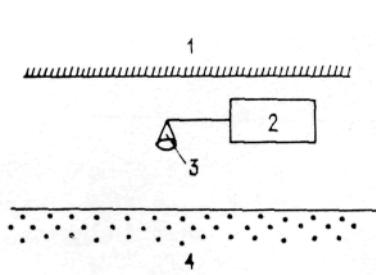


Fig. 1

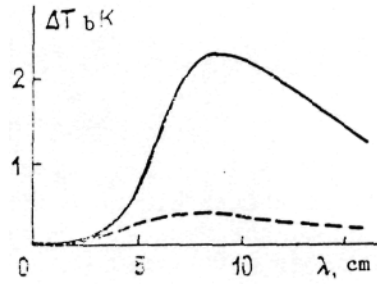


Fig. 2

Fig. 1. Soil measurement diagram: 1) metal shielding; 2) radiometer; 3) horn antenna; 4) soil.

Fig. 2. The difference  $\Delta T_b$  between the brightness temperatures, calculated both without and with consideration of scattering  $\sigma_e^2 = 0.5$ ,  $\epsilon = 6 - i0.1$ ,  $l = 0.5$  cm,  $T(z) = 275 - 15 \exp(z/30)$ . The solid line represents measurements without shielding, while the dashed line represents measurements with shielding.

with a given correlation function  $\psi_\epsilon(\tau) = \sigma_\epsilon^2 \exp(-\tau^2/2l^2)$ , such that  $\epsilon''$ ,  $\sigma_\epsilon^2 \ll \epsilon'$ . The brightness temperature of such a medium is described by the transfer equation

$$\mu \frac{d}{d\tau} T_b(\tau, \mu) + T_b(\tau, \mu) - \omega_0 \int_{-1}^1 d\mu' \hat{P}(\mu, \mu') T_b(\tau, \mu') = (1 - \omega_0) I^0 T(\tau) \quad (1)$$

with the boundary condition

$$T_b(0, \mu) |_{\mu > 0} = \hat{R} T_b(0, -\mu), \quad (2)$$

where  $[T_E, T_H]$  vector of the brightness temperature, whose components correspond to the horizontal (E) and vertical (H) polarizations;  $\mu = \cos \theta$ ,  $\mu' = \cos \theta'$ ;  $\theta$  and  $\theta'$  are angles reckoned from the  $z$  axis;  $\hat{P}$  is a scattering matrix  $2 \times 2$ ;  $\tau = (\gamma + \alpha)z$ ,  $\omega_0 = \alpha / (\alpha + \gamma)$ , where  $\alpha$  and  $\gamma$  are, respectively, the coefficients of scattering and absorption in the medium;  $I^0$  is a unit matrix. The diagonal matrix of reflection coefficients  $R$  where diagonal elements  $R_E$  and  $R_H$  in the absence of shielding are the Fresnel coefficients with respect to power, while in the presence of the shielding we have  $R_E = R_H = 1$ .

In the vertical direction  $T_E(\tau, -1) = T_H(\tau, -1) = T_b(\tau, -1)$ , so that the measured brightness temperature is therefore

$$T_b = (1 - R) T_b(0, -1), \quad (3)$$

where  $R = \left| \frac{1 - \sqrt{\epsilon_0}}{1 + \sqrt{\epsilon_0}} \right|^2$  in the absence of shielding and  $R = 0$  in the presence of shielding.

Equation (1) was solved by the method proposed in [6] for the case  $u_0 \ll 1$ .

Figure 2 shows the results obtained in calculating the difference in the brightness temperatures  $\Delta T_b$  both with and without consideration of scattering in the case of a model temperature profile  $T(z) = T_0 - \Delta T \exp(-z/z_0)$ , and also both with and without shielding. We can see that shielding makes it possible considerably (by a factor of 8-10) to reduce the extent to which brightness temperature in the medium is reduced, and here the quantity  $\Delta T < 0.3$  K is of the same order of magnitude as the errors in the measurement of  $\delta T_b$ , tolerated in the solution of the inverse problem. Let us take note of the fact that the effect exerted by scattering, as can be seen from Fig. 2, is estimated on the basis of the maximum. Moreover, shielding makes it possible completely to offset the influence of the reflection coefficient  $R$  on the radio emission of the medium. This enables us to avoid those errors associated with imprecise knowledge of the quantity  $R$  whose variation with changes in humidity and composition of the soil lead to fluctuations in  $T_b$  of up to 30-40 K [1].

In the foregoing we have been looking at an idealized measurement scheme. In actual practice, compensation is achieved by satisfying a number of conditions. If we take into consideration that with  $n$ -multiple reflections the magnitude of the uncompensated brightness temperature is on the order of  $R^n$ , then the dimensions of the shielding must be

$$L \geq \frac{\lambda}{d_a} \left( h_s + h_a + \frac{1}{\gamma} \right) \left( \ln \frac{\delta T_b}{T_b} / \ln R - 1 \right), \quad (4)$$

where  $h_s$  is the height of the shield above the ground;  $d_a$  and  $h_a$  are the dimensions of the aperture and the height of the receiving antenna. When relationship (4) has been satisfied, the compensated error does not exceed the measurement error  $\delta T_b$ .

To avoid having the nonzero dimension of the antenna affect the shielding, it is necessary that

$$d_a \ll \lambda h_a \quad (5)$$

For noncoherent combination of intensities in the case of rereflection it is necessary that

$$h_a > c/2\Delta\nu, \quad (6)$$

where  $c$  is the speed of light and  $\Delta\nu$  is the radiometer band. In the case of soil it is enough to have one or two re-reflections, and conditions (A)-(6) are satisfied if  $h_s \sim h_a \sim 1$  m,  $L = 2$  m for typical parameters of the radiometry system. Thus, the developed measurement I method allows us to interpret the measured brightness temperatures of the medium on the basis of the following equation:

$$T_b(\lambda) = \int_{-\infty}^0 T(z) \gamma(\lambda) e^{\gamma z} dz, \quad (7)$$

valid for the case in which  $\gamma$  is independent of  $z$ , i.e., for uniform and, in particular (see [1]), uniform moist soils (variations in  $\gamma$  should lead to no variations in  $T_b$  greater than  $\delta T_b$ ).

The absolute calibration of the radiometric system is accomplished by means of two identical absorbing bodies with different temperatures (the temperature of melting ice and the outside air). Shielding significantly simplifies the calibration, since there is no need to take into consideration the coefficient of reflection for the materials being calibrated. The accuracy in the measurement of  $T_b$  for the soil, by means of the method developed here, is estimated to be  $-0.2-0.3$  K.

2. Solution of the Inverse Problem. Equation (7) represents a linear integral Fredholm equation of the first kind and is an incorrectly formulated problem in the sense of [7]. For its solution it is necessary to draw on considerable a priori information regarding the properties of the exact solution. We made use of the Tikhonov regularization method in the form of a principle of generalized-discrepancy [7]. If we take into consideration that we have already repeatedly used this method to solve inverse problems leading to the Fredholm equation of the first kind [4, 8-10], including those near the similar physical situations of reproducing the subsurface temperature profile of a water medium [4] and of biological media [10], we will cite only certain of the general conclusions and note the specific aspects of soil probing.

In solving this incorrect problem, questions dealing with the relationship between measurement accuracy and reproduction, as well as the optimum selection of wavelengths, are solved on the basis of numerical simulation, since everything depends on the specific form of the core and class of the reproduced distributions. Monotonic functions and functions with a single maximum, uniformly distributed over the integration interval, are reproduced in the case of soil probing with an accuracy of  $0.5-2$  K from measurements at three to four wavelengths, where the thickness of the skin layer  $d_s = 1/\gamma$  is as uniform as possible in its coverage of the depth of the reproduction interval. The measurement accuracy must be  $0.2-0.3$  K. Let us note that the Tikhonov method for problems of reproducing temperature profiles has a particular informal sense, since the quantity  $dT/dz$  in the regularization functional (see, for example, [4]), accurate to the thermal-conductivity constant, represents the flow of heat, thus making it possible in the solution of the problem to use independent information with regard to the distribution of the heat flow.

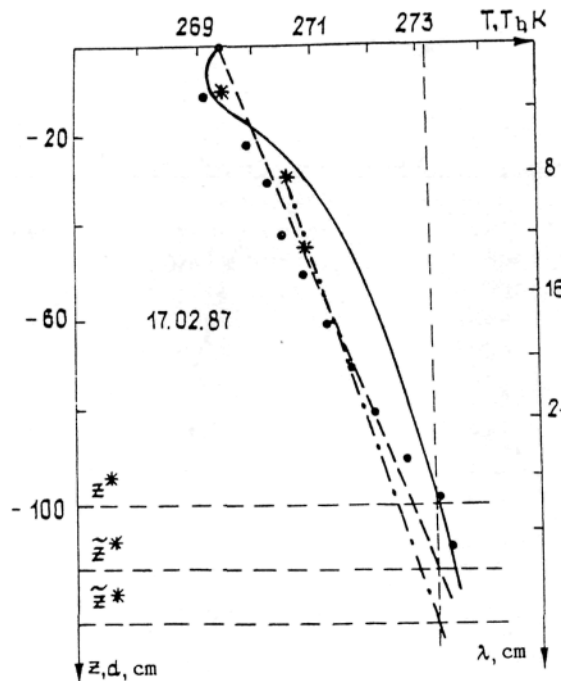


Fig. 3. Results from radiometry and contact measurements of the soil. The points identify the contact measurements of temperature as functions of the depth. The asterisks represent the brightness temperatures of the soil at wavelengths of 3, 9, and 13 cm, shown as functions of the skin-layer depth  $d$ . The solid curve is the profile of  $T(z)$ , reproduced by the Tikhonov method. The dashed line represents the reproduction of  $T(z)$  and  $z^*$  with a single-wave method; the dot-dash line reflects a two-wave method.

3. Superhigh-Frequency Probing of Frozen Soil. In February-March 1987 measurements of the thermal radio emissions of frozen soil were carried out on wavelengths of 3, 9, and 13 cm. Contact measurements of soil temperatures at various depths were simultaneously carried out, with separations of 10 cm, which made it possible to monitor the freezing depth  $z^*$  which was determined from the condition  $T(z^*) = 0$ .

For various profiles of  $T(z)$ , determined by the contact method, we calculated the values of  $T_b$ , with the absorption coefficients  $\gamma(\lambda)$  chosen so that the theoretical values of  $T_b$  coincided with the values measured for each wavelength. For the thickness of the skin layer  $d_{sk} = 1/\gamma$ , using the method of least squares, we obtained the following relationship

$$d_{sk} = (3.25 \pm 0.2)\lambda, \quad (8)$$

which showed that the frozen soil was similar in properties to a dielectric without dispersion.

The variations in  $T_b(\lambda)$ , corresponding to indeterminacy in  $d_{sk}$  in (8), turn out to be smaller than the error in the measurement of  $T_b$ . The absorption factor  $\gamma$  on the basis of (8), was used in the subsequent experiments to reproduce the  $T(z)$  profile from solution of Eq. (7). Figure 3 gives an example of reproduction involving utilization of the natural a priori limitation  $T(z) < 273.5$  K (solid curve). The extent to which the soil was frozen through its depth was determined from the condition  $T(z^*) = 0$  on the basis of the reproduced profile.

The results from the research carried out here demonstrated that the dielectric parameters of the frozen soil during the winter period are exceedingly stable and can be determined from data of one-time measurements at reference points in segments with a uniform soil character such as, for example, by the proper selection of a "divining rod" [11]. Another possibility of determining  $\epsilon$  of the frozen soil is involved with the development of efforts to establish the empirical relationships analogous to those obtained earlier for soils, in the case of positive temperatures (see [12]), thus making it possible to calculate the dielectric parameters in their dependence on the composition of the soil.

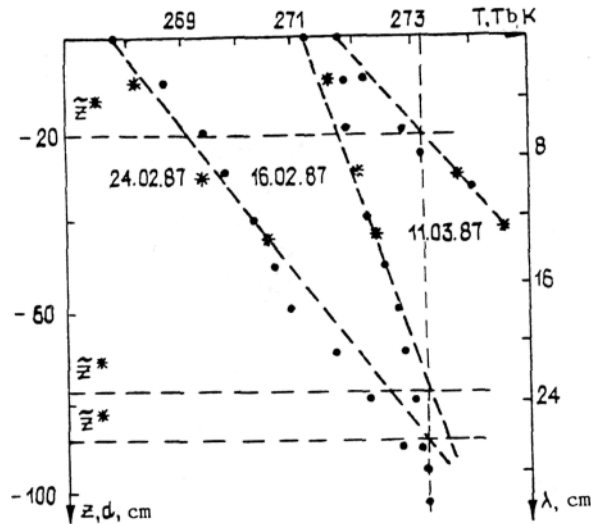


Fig. 4. Results from radiometry probing of frozen soil for three days of observation with single-wave method. Notation as in Fig. 3.

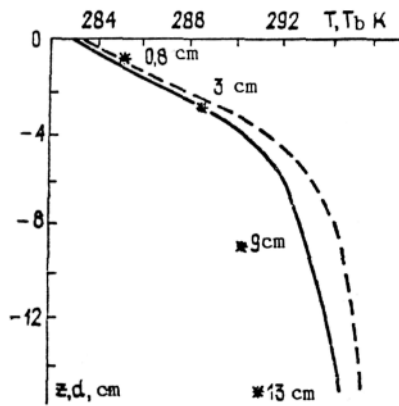


Fig. 5

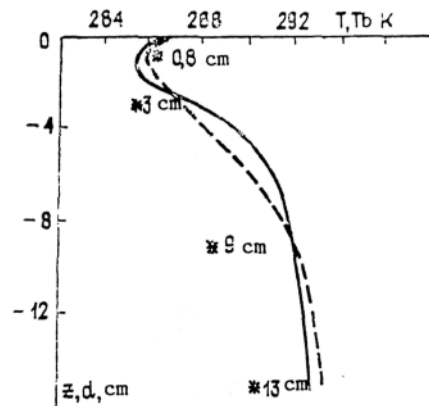


Fig. 6

Fig. 5. Reproduction of surface soil temperature profile at 7<sup>h</sup>30<sup>min</sup> on October 6, 1986. The solid curve is the profile of  $T(z)$ , reproduced from the  $T_b$  measurements in accordance with the Tikhonov method [the values of  $T_b(\lambda)$  are identified by asterisks in dimensions of the skin-layer depth  $d(\lambda)$ ; the dashed line represents the  $T(z)$  profile taken from the solution of the heat-conduction equation].

Fig. 6. The same as in Fig. 5 for measurements at 12<sup>h</sup>20<sup>m</sup> on October 6, 1986.

In order to reproduce the  $T(z)$  profile out of the  $T_b(\lambda)$  measurements, in addition to the above-cited general approach to the solution of the inverse problem, we can take advantage of the circumstance that for a frozen soil or for ice on the surface of the water the  $T(z)$  profile is usually close to linear. Indeed, the lower boundary of the frozen soil is stable, owing to the inertia of the phase-transition process and is at temperature 0. If the temperature at the upper boundary of the layer is constant for a prolonged period of time, a linear distribution of temperature is established, and this corresponds to the steady-state solution of the heat-conduction equation

$$\frac{\partial T}{\partial t}(z, t) = a^2 \frac{\partial^2 T}{\partial z^2}(z, t), \quad (9)$$

which has the form

$$T(z) = T_1 + \frac{T_2 - T_1}{z^*} z, \quad (10)$$

where  $T_1$  and  $T_2$  are the temperatures at the upper and lower boundaries of the layer,  $z^*$  is the depth of freezing [ $T(z^*) = T_2 = 0$ ]. Estimates show that for  $z^* \sim 1$  m the time required to establish the linear profile amounts to more than a day, i.e., rapid weather changes may lead to nonlinearity in  $T(z)$ . However, we should take into consideration that in the presence of a snow cover more than 20 cm thick, owing to the limited conduction of heat in the snow [ $a^2 \sim (0.5-1) \cdot 10^{-3}$  cm<sup>2</sup>/sec] the daily variations in temperature at the soil surface level are insignificant. (The presence of a dry snow cover does not interfere with the radiometric measurements, since in the range under consideration the snow is virtually transparent to radio emissions [13].) With  $z^* < 20-30$  cm,  $T(z)$  can track the diurnal dynamics without any loss of linearity. In actual practice it is not difficult to evaluate the extent to which the conditions of linearity in  $T(z)$  have been satisfied. Additional information regarding the linearity of  $T(z)$  is provided by the linearity of the measured function  $T_b(\lambda)$ , since the linear profile  $T(z)$  is an eigenfunction (7) and the brightness temperatures are equal to the values of  $T(z)$  at depths of  $z = -d_{sk}$ . Throughout the measurement period, the observed  $T(z)$  profiles, as a rule, were nearly linear.

For a linear profile such as (10), in the determination of  $T(z)$  and  $z^*$  it is possible to avoid solution of the incorrect problem by using the Tikhonov method on a computer with data of multi-frequency measurements. A single frequency method of evaluating  $z^*$  is possible with the additional utilization of the measured value of the surface temperature  $T_0$

$$\tilde{z}^* = \frac{d_{sk}}{T_b/T_0 - 1} \quad (11)$$

and a two-frequency method in which there is no need to measure  $T_0$ :

$$\tilde{z}^* = \frac{(T_{b1}/T_{b2})d_{sk2} - d_{sk1}}{1 - (T_{b1}/T_{b2})}, \quad (12)$$

$T_0$ ,  $T_{b1}$ ,  $T_{b2}$  (°C). Algorithms (11) and (12) are based on reproduction of the linear  $T(z)$  profile on the basis of two points whose coordinates in the  $T, z$  plane are:  $(T_b, -d_{sk})$  and  $(T_0, 0)$  in the first case and  $(T_{b1}, -d_{sk1})$ ,  $(T_{b2}, -d_{sk2})$  in the second case. Figure 3 shows results from the determination of  $T(z)$  and  $z^*$  according to (11) and (12) in comparison to the Tikhonov method. The accuracy in the reproduction of  $T(z)$  by the Tikhonov method in this case diminishes slightly as the depth increases, since the thickness  $d_{sk}$  of the skin layer at the maximum wavelength (13 cm) is considerably smaller than the depth of the probed layer. The profiles reproduced by these various methods showed good agreement with contact measurement data.

Figure 4 shows results from the determination of  $z^*$  according to (11) for three different days of observation, and we also see the results obtained on March 11, 1987 from the measurements of a segment covered by deep snow. We can see that the presence of the snow cover markedly reduces the depth of soil freezing. Let us note that for this example the thickness of the skin layer at  $\lambda = 9$  and  $\lambda = 13$  cm exceeds the thickness of the frozen layer and the change in  $y$  (not taken into consideration here) in the phase-transition zone makes itself felt on the result. Nevertheless, the estimate  $z^* = -20.6$  cm turned out to be close to the real value. The results show that the microwave radiometric method allows us to determine the depth of soil freezing with an accuracy of 15-20%.

This method developed here was used also to determine the thickness of the ice cover in reservoirs, in particular, for the case of a limited ice thickness (on the order of several centimeters), which is difficult to do with the radiolocation method [14].

4. Radiometric Probing of the Diurnal Temperature Dynamics of the Soil. Soil brightness temperatures were measured over a period of three days at wavelengths of 0.8, 3, 9, and 13 cm in October 1986, at the NIRFI Karadag Test Range (on the southeastern shore of the Crimean Peninsula), and these were accompanied with simultaneous contact measurements of soil surface temperatures  $T_0(t)$ . The moisture content of the soil, determined by means of a thermostat-gravimetric method, came to  $14 \pm 2\%$ , with provision made for variations in depth. According to [12], estimates were obtained for the parameters  $\varepsilon'$ ,  $\varepsilon''$ , and  $\gamma(\lambda)$ . In particular, for  $\lambda = 3$  cm,  $\varepsilon' = 5$ ,  $\varepsilon'' = 0.4$  the thickness of the skin layer is  $d_{sk} \approx 3$  cm. With  $\lambda = 13$  cm,  $d_{sk} = 15$  cm. We can see that owing to the effect of the moisture contained within the soil, the thickness of the skin layer is markedly reduced in comparison with the frozen soil.

Figures 5 and 6 show the results of the reproduction of  $T(z)$  for two instants of time in the diurnal cycle, corresponding to 7<sup>h</sup>30<sup>m</sup> and 12<sup>h</sup>20<sup>m</sup> local time on October 6, 1986, obtained by solution of inverse problem (7) by the Tikhonov method. The solution was sought in the form of deviations from the function  $T^{\circ}(z) = 20^{\circ}\text{C}$ . The reproduced profiles are compared with the  $T(z)$  profiles, obtained from the solution of the heat-conduction equation (9) from the measurements of surface temperature  $T_0(t)$  evolution. The heat-conduction coefficient  $a^2$  as a function of the type of soil and its moisture content are determined in accordance with [15]. Equation (9) has the following solution (see, for example, [15]):

$$T(z, t) = \int_{-\infty}^t -\frac{zT_0(\tau)}{\sqrt{4\pi a^2(t-\tau)^3}} \exp\left[-\frac{z^2}{4a^2(t-\tau)}\right] d\tau. \quad (13)$$

It follows from (13) that the maximum contribution to the temperature at the depth  $z$  at the instant of time  $t$  is made by the temperature  $T_0(\tau_m)$  at the instant  $\tau_m$ , separated from the earlier instant  $t$  by

$$t - \tau_m = z^2 / 6a^2 \quad (14)$$

Estimates based on (14) and calculations according to (13) show that in the case under consideration the diurnal dynamics in  $T(z)$  prevail in a layer at a depth of ~15-20 cm.

The results shown in Figs. 5 and 6 show that we have good agreement between the profiles obtained with a variety of approaches. The brightness temperatures are shown in the figures as functions of the skin-layer thickness for each wavelength.

The profiles in Figs. 5 and 6 reflect the specific characteristics of the diurnal dynamics in  $T(z)$ . Figure 5 shows a reproduction of the profile corresponding to pronounced nighttime cooling of the soil's surface layer, while Fig. 6 shows the same profile after a lapse of several hours, at the onset of the daylight heating of the soil, which leads to the formation of an inversion in  $T(z)$  in the layer near the surface.

The skin-layer depths  $d_{sk}(\lambda)$  for these wavelengths uniformly cover the layer subject to the diurnal dynamics, thus ensuring high-quality reproduction (no less than 20% of the temperature drop across the profile).

The authors are grateful to D. M. Gordeev for his assistance in the measurements conducted at the Karadag Test Range and to K. S. Stankevich for his useful comments.

#### LITERATURE CITED

1. A. M. Shutko, SHF Radiometry of Water Surfaces and Soils [in Russian], Nauka, Moscow (1986).
2. K. Ya. Kondrat'ev, Yu. M. Timofeev, and V. M. Shul'gina, Dokl. Akad. Nauk SSSR, 194, No. 6, 1313 (1970).
3. K. Ya. Kondrat'ev and V. M. Shul'gina, Dokl. Akad. Nauk SSSR, 200, No. 1, 88 (1971).
4. K. P. Gaikovich, A. N. Reznik, M. I. Sumin, and R. V. Troitskii, Izv. Akad. Nauk SSSR, Ser. FAO, 23, No. 7, 761 (1987).
5. M. L. Levin and S. M. Rytov, The Theory of Equilibrium Thermal Fluctuations in Electrodynamics [in Russian], Nauka, Moscow (1967).
6. A. N. Reznik, Izv. Vyssh. Uchebn. Zaved., Radiofiz., 26, No. 4, 506 (1983).
7. A. N. Tikhonov, A. V. Goncharskii, V. V. Stepanov, and A. G. Yagola, Regularizing Algorithms and A Priori Information [in Russian], Nauka, Moscow (1983).
8. N. A. Vasilenko, K. P. Gaikovich, and M. I. Sumin, Dokl. Akad. Nauk SSSR, 290, No. 6, 1332 (1986).
9. K. P. Gaikovich and M. I. Sumin, in: Abstracts of the 7th AH-Union Conference on Radiometeorology, Moscow (1986), p. 6.
10. K. P. Gaikovich, M. I. Sumin, and R. V. Troitskii, Izv. Vyssh. Uchebn. Zaved., Radiofiz., 31, No. 9, 1104 (1988).
11. A. Sihvola and M. Tivri, IEEE Trans. Geosci. Remote Sensing, 24, No. 5, 717 (1986).
12. M. T. Hallikainen, F. T. Ulaby, M. A. El-Rayes, and L. Wu, IEEE Trans. Geosci. Remote Sensing, 23, No. 1, 25 (1985).
13. M. T. Hallikainen and F. T. Ulaby, IEEE Trans. Anten. Propag., 34, No. 11, 1329 (1986).
14. M. I. Finkel'shtein, È. I. Lazarev, and A. N. Chizhov, Airborne Radar Measurements of Rivers, Lakes, and Reservoirs [in Russian], Gidrometeoizdat, Leningrad (1986).
15. A. F. Chudnovskii, The Thermophysics of Soils [in Russian], Nauka, Moscow (1976). 1088.